Supplementary Information

Harrington J et al.

Human iPSC-Derived Lens Organoids Recapitulate Lens Development and Morphogenesis In Vitro

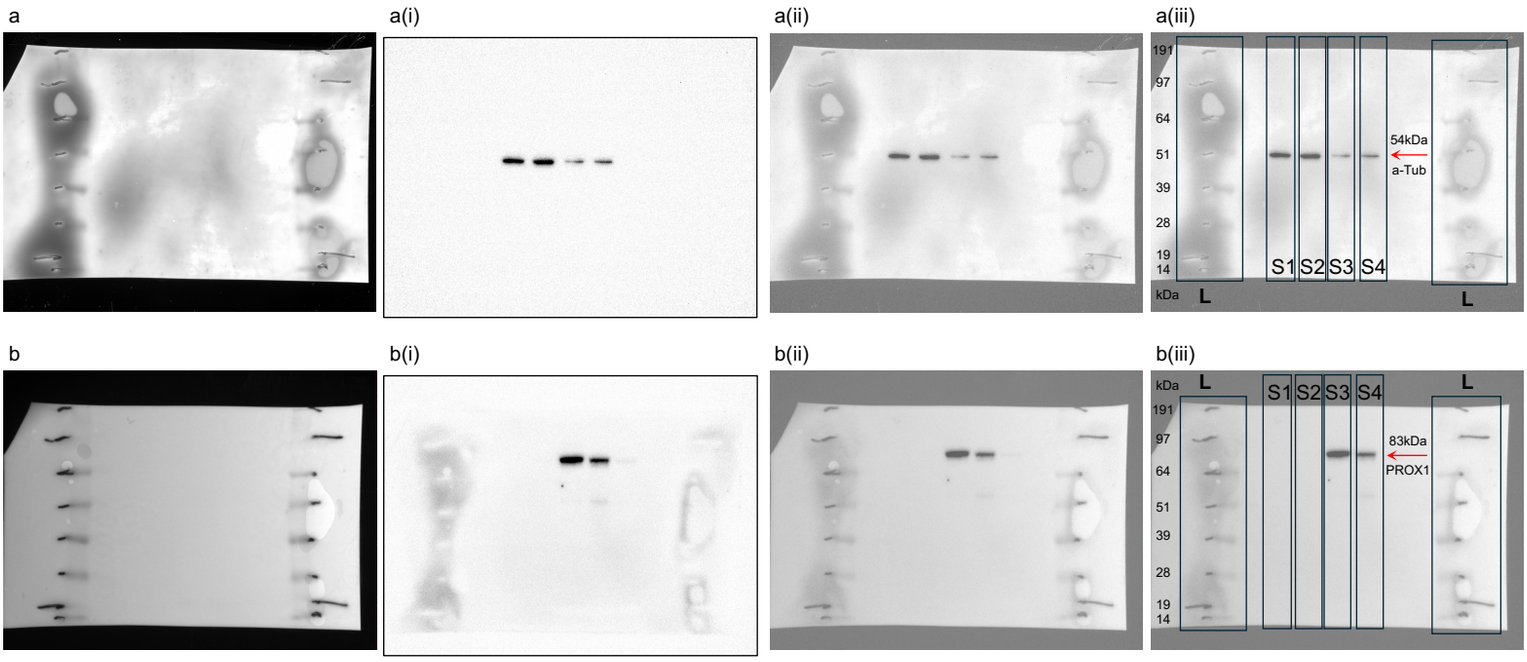

Supp. Fig. 1: Western blot (WB) of hiPSC and LOM (lens optimised medium) colony cultures before and after differentiation. a Raw WB membrane light-image with penned-lines probed for alpha-Tubulin. **a(i)** WB membrane probed for alpha-Tubulin house-keeping reference protein under chemiluminescence was present in hiPSCs after 10 days culture in StemFit®AK02N medium (samples S1 and S2) and after 8 weeks in LOM (samples S3 and S4). **a(ii)** Raw WB membrane light-image and chemiluminescence image overlaid. **a(iii)** Alpha-tubulin protein was detected alongside ladder (L) at the expected molecular weight of 52 kDa in all four samples (S1-S4). **b** Raw WB membrane light-image with penned-lines probed for PROX1. **b(i)** WB membrane probed for PROX1 protein under chemiluminescence was absent in hiPSCs after 10 days culture in StemFit®AK02N medium (samples 1 and 2) and present after 8 weeks in LOM (samples 3 and 4). **b(ii)** Raw WB membrane light-image and chemiluminescence image overlaid. **b(iii)** PROX1 protein was detected alongside ladder (L) at the expected molecular weight of 83 kDa, after 8 weeks in LOM samples (S3-S4) and absent in hiPSCs after 10 days culture in StemFit®AK02N medium samples (S1 and S2). *n*=2 independent biological replicates.

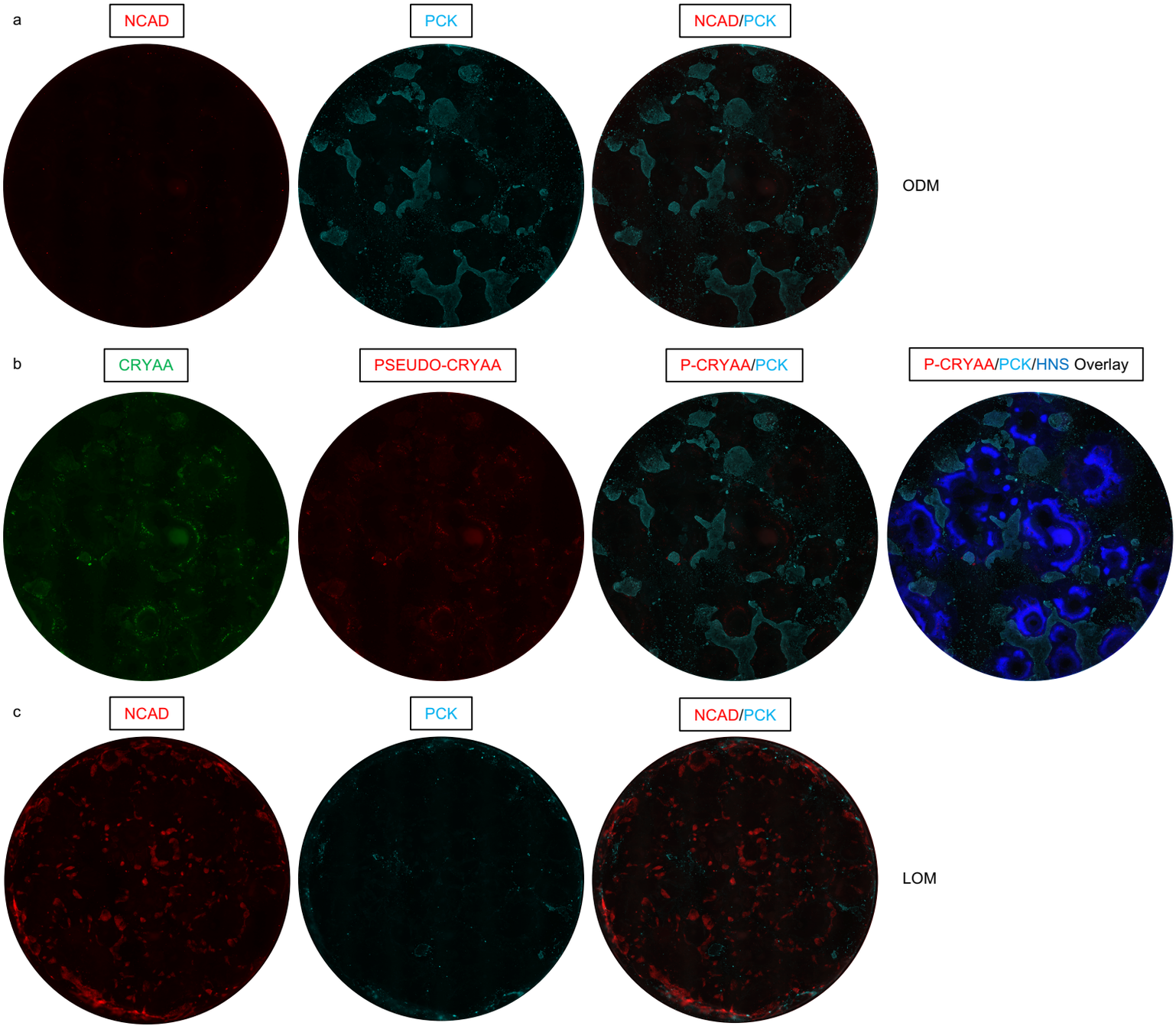

Supp. Fig. 2: Immunofluorescence within whole-well ODM (ocular differentiation medium) and LOM (lens optimised medium) cultures at 8 weeks differentiation displayed protein restrictions for lentoids and colony zones. a NCAD (red) was absent in ODM and pan-cytokeratin (PCK; cyan) was strongly restricted at SEAM periphery (*i.e*. zone 2-3 border outwards), as confirmed by localised CRYAA and nuclei (**b**). **c** NCAD (red) was strongly restricted to lentoids in LOM and PCK (cyan) was limitedly present at SEAM and lentoid periphery (*i.e*. zone 2L-3 border outwards). PCK marker potentially represented cells/tissues as follows: CK1 (epidermis (eyelid)), CK4 and CK13 (conjunctiva), CK5 (basal corneal epithelium; lens epithelium) and CK8 (foetal lens epithelium). Hoechst nuclei in images are blue (HNS). *n*=3 independent biological replicates.

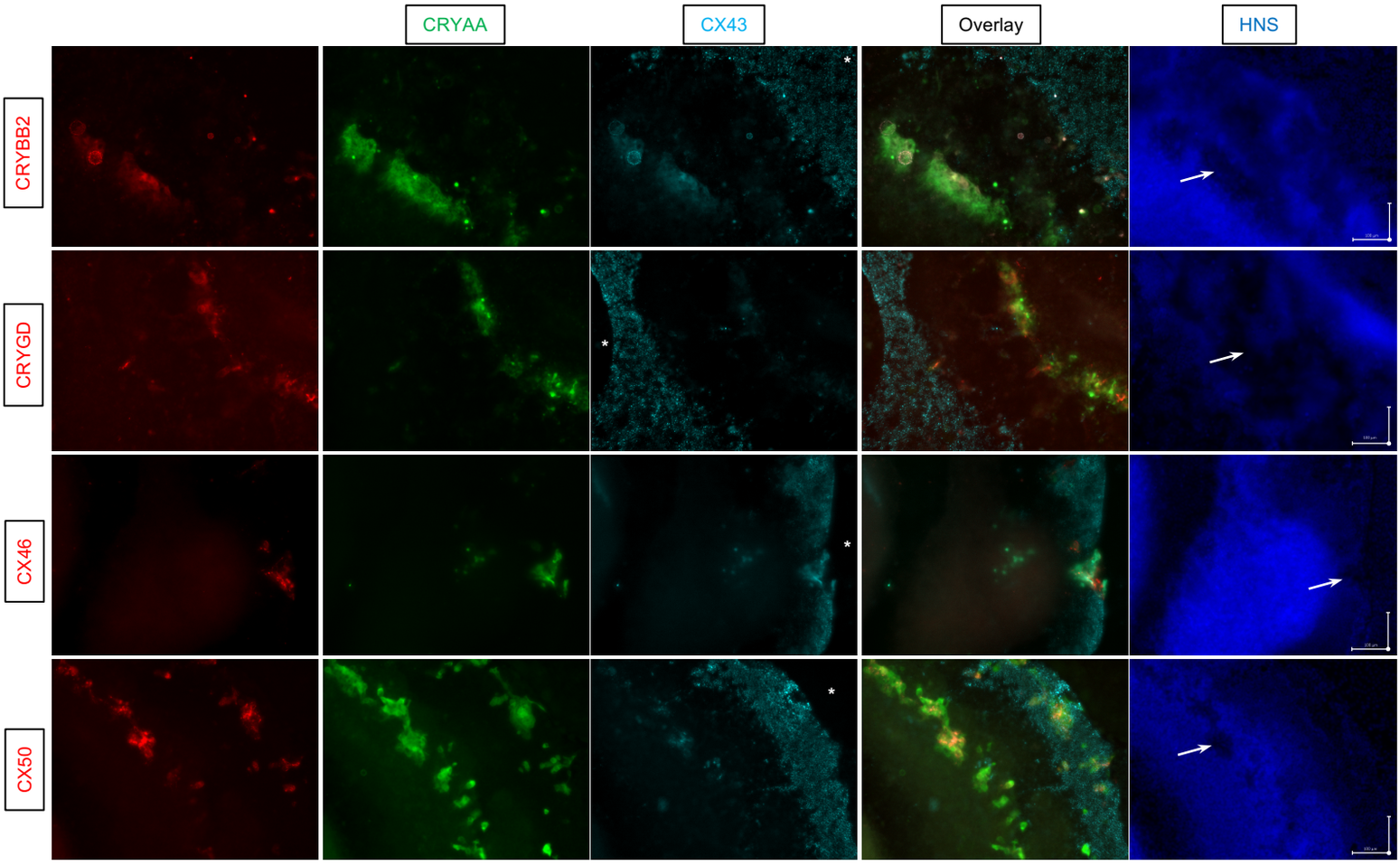

Supp. Fig. 3: Immunofluorescent localisation of mature lens-related markers within ODM (ocular differentiation medium) culture at 8-weeks differentiation. Crystallin CRYAA (green) and connexin CX43 (cyan) were the most abundantly localised proteins. CX43 (representative of lens-presumed epithelium) was punctate and clearly demarcated the border between lens and cornea tissues (zones 2 and 3, respectively; refer to Figure 1), and white asterisks indicate corneal zone 3 as opposing side to SEAM colony centre. Crystallin CRYAA indicated co-localisation with all crystallins CRYAB, CRYBB2 (low-levels) and CRYGD, as-well-as connexins CX46 (low-levels) and CX50 within multiple small lentoids, as highlighted by overlay images. Nuclei (HNS; blue) were generally less and weaker compared to non-lentoid areas (white arrow). ODM connexin abundances (CX43>CX50>CX46). Scalebars = 100μm. *n*=3 independent biological replicates.

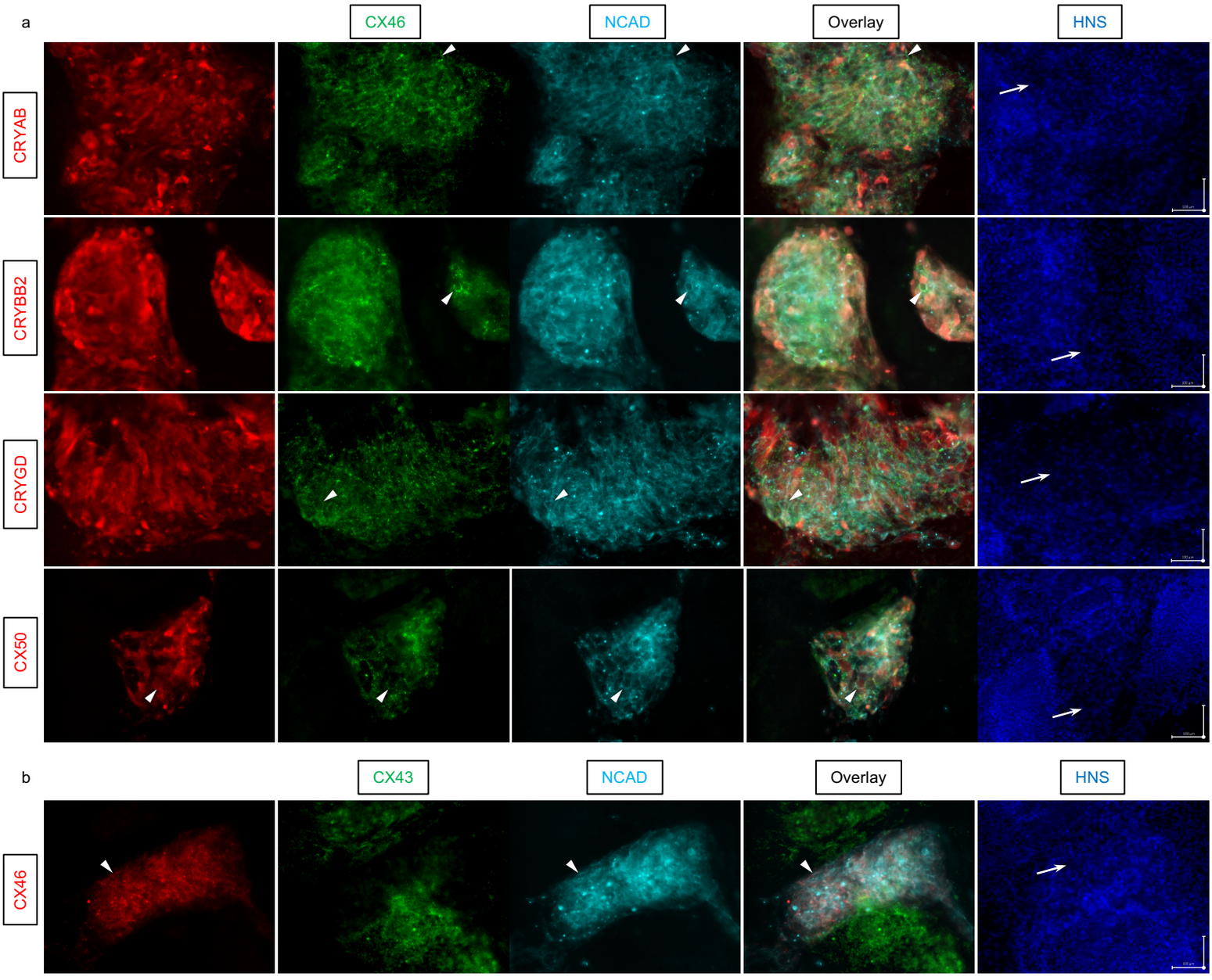

Supp. Fig. 4: Immunofluorescent localisation of mature lens-related markers within LOM (lens optimised medium) cultures at 8-weeks differentiation. a Both connexin CX46 (green) and CX50 (red), and cadherin NCAD (cyan), were highly localised with crystallins CRYAB, CRYBB2 and CRYGD and connexin CX50 (red), and were restricted to lentoid bodies (LBs) as highlighted by overlay images. White triangles highlight examples of connexin (CX46 and CX50) punctation along NCAD membrane. **b** Epithelial connexin CX43 (green; representative of lens-presumed epithelium pool) was found in close but restricted association with lens-related connexin 46 (red) and displayed limited to no overlap, nor with NCAD (cyan). Nuclei (HNS; blue) were generally less and weaker compared to non-lentoid areas (white arrow). Scalebars = 100μm. *n*=3 independent biological replicates.

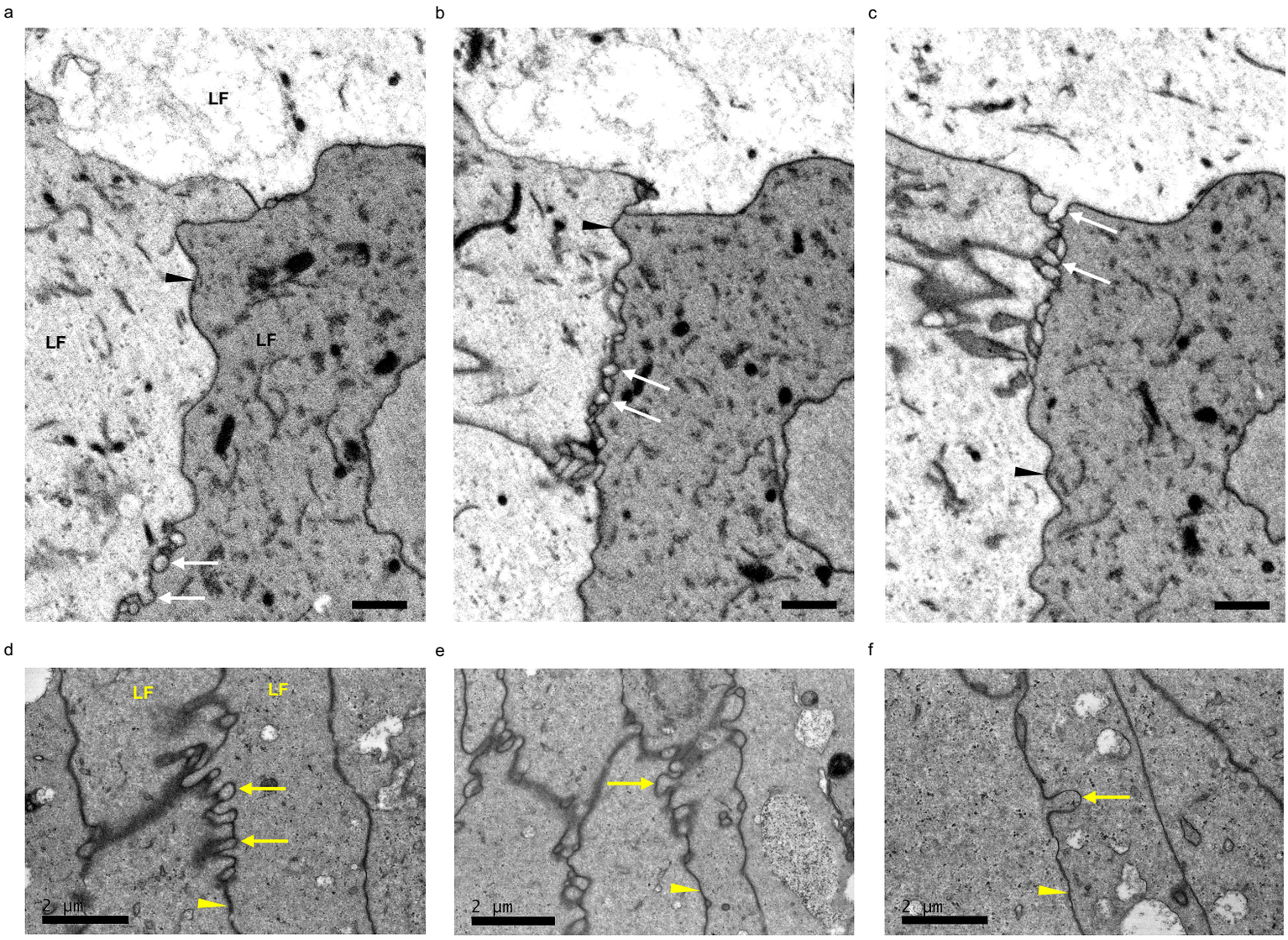

Supp. Fig. 5: Serial Block-Face Scanning Electron Microscopy (SBF-SEM) and Transmission Electron Microscopy (TEM) of LOM (lens optimised medium) culture after 8 weeks differentiation displayed interdigitation features. a, **b** and **c** Flythrough ROI (regions of interest) of LOM lentoid detailed presumed cortical lens fiber (LF) cells with their intercellular membranes (black triangle) and membrane interdigitations (white arrow). **d**, **e** and **f** Compared to human foetal lens tissue at 20-weeks gestation, displaying LF cells, intercellular membranes (yellow triangle) and interlocking ball-and-sockets (yellow arrow), the LOM lentoid interdigitations were reminiscent of typical ball-and-socket structures found in vertebrate lenses, observed by size and morphology. See supplementary video MINT (SF Movie 5) for LOM membrane interdigitations flythrough. Scalebars = 1μm (**a**–**c**) and 2μm (**d**–**f**). SBF-SEM (**a**–**c**) and TEM (**d**–**f**). SBF-SEM and TEM, *n*=1 independent biological replicates (2–3 ROIs). Human lens TEM images courtesy of Robert D. Young (**d**–**f**).

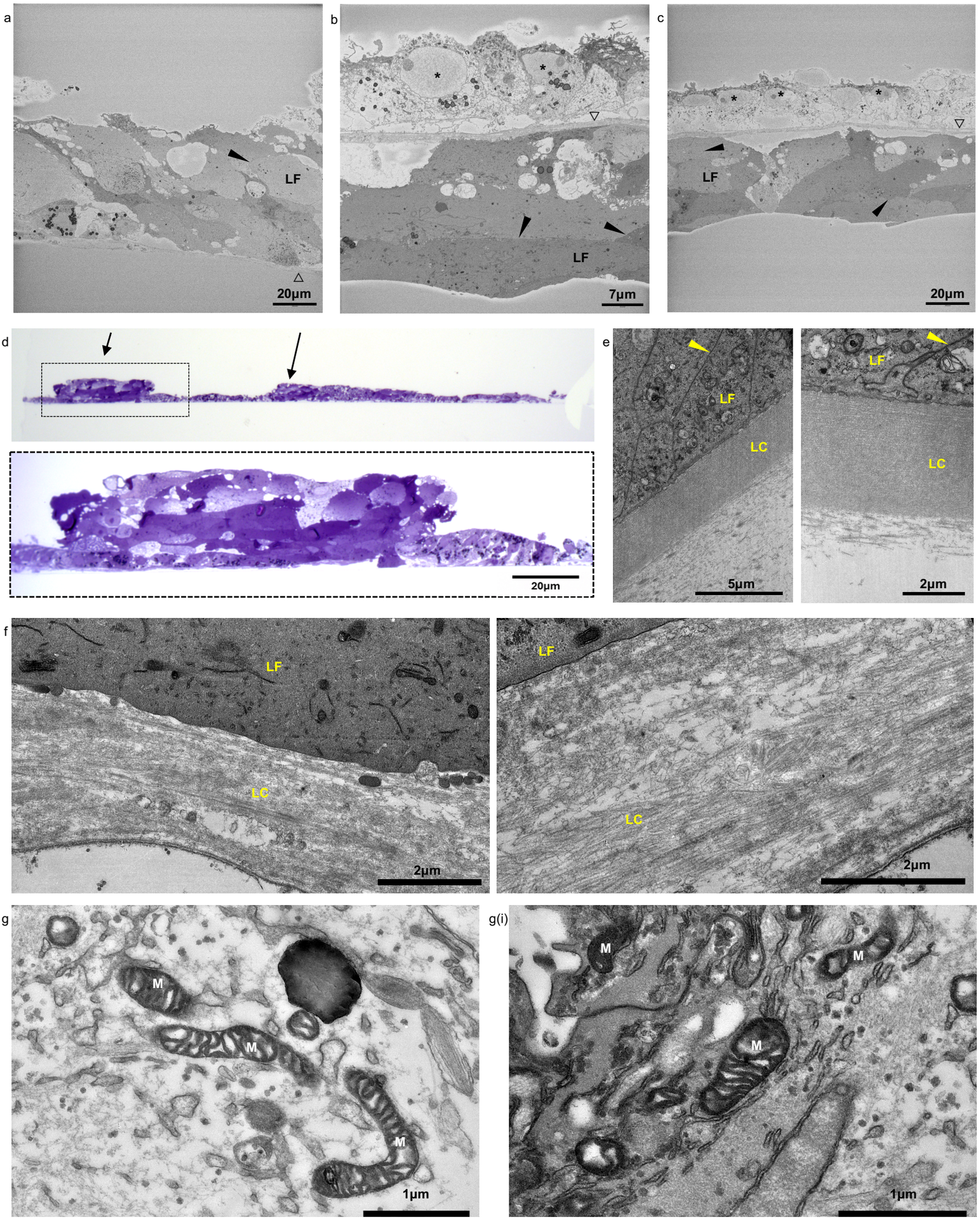

Supp. Fig. 6: Serial Block-Face Scanning Electron Microscopy (SBF-SEM) and Transmission Electron Microscopy (TEM) of LOM (lens optimised medium) culture after 8 weeks differentiation displayed human lens tissue features. SBF-SEM detailed additional ROIs (regions of interest) within LOM culture as lenticular ocular-population areas, distinguishing lentoids with presumed cortical lens fiber (LF) cells, LF cell intercellular membranes (black triangle) and lamellar basement membranes as presumed lens capsule (black triangle outline), and all distinct from simple rounded and nucleated non-lentoid (NL) cells (black asterisk) (a–c). **a** SBF-SEM of a second lentoid ROI (for first ROI, see Figure 7a). **b**, **c** SBF-SEM of a first and second lentoid ROI with NL cells (top) external to lens capsule; as expected within an ocular-population tissue culture. **d** Toluidine blue staining highlighted lens fiber cells of whole LOM organoids that exhibited localised multilayered organisation (black arrows), amongst surrounding areas of other simple ocular NL cells; magnified view in black line-dashed box. **e** TEM of human foetal lens at 20-weeks gestation showed cortical LF cells (top) with intercellular membranes (yellow triangle) and the fibrillar lens capsule (LC) lamella (bottom); a magnified view given as righthand image. **f** TEM of LOM lentoid showed presumed cortical LF cells (top) and a fibril lamellae of the presumed lens capsule (LC, bottom), which are comparable features as shown by human lens (**e**); a magnified view given as righthand image. **g**, **g(i)** TEM of presumed lens epithelial (LE) cells, which were dense with organelles such as metabolically active mitochondria (M). See supplementary videos LOM (SF Movies 3 and 4) and LOM_NL (SF Movies 6 and 7) for more detailed reconstructions of each sample (Flythrough and 3D Render, respectively). Note: in video LOM Flythrough (SF Movie 4), some nucleate and organelle dense cells (bottom right) between LF cells and presumed LC that possibly represent lens epithelia (as seen in Figure 7e). Note: all SEM samples contained unidentifiable dark electron dense granules but possibly represent lysosomes. SBF-SEM (**a**–**c**), *n*=2 independent biological replicates (2–3 ROIs). TEM (**e**–**g(i)**), *n*=1 independent biological replicates (2–3 ROIs). Human lens TEM images courtesy of Robert D. Young (**e**).

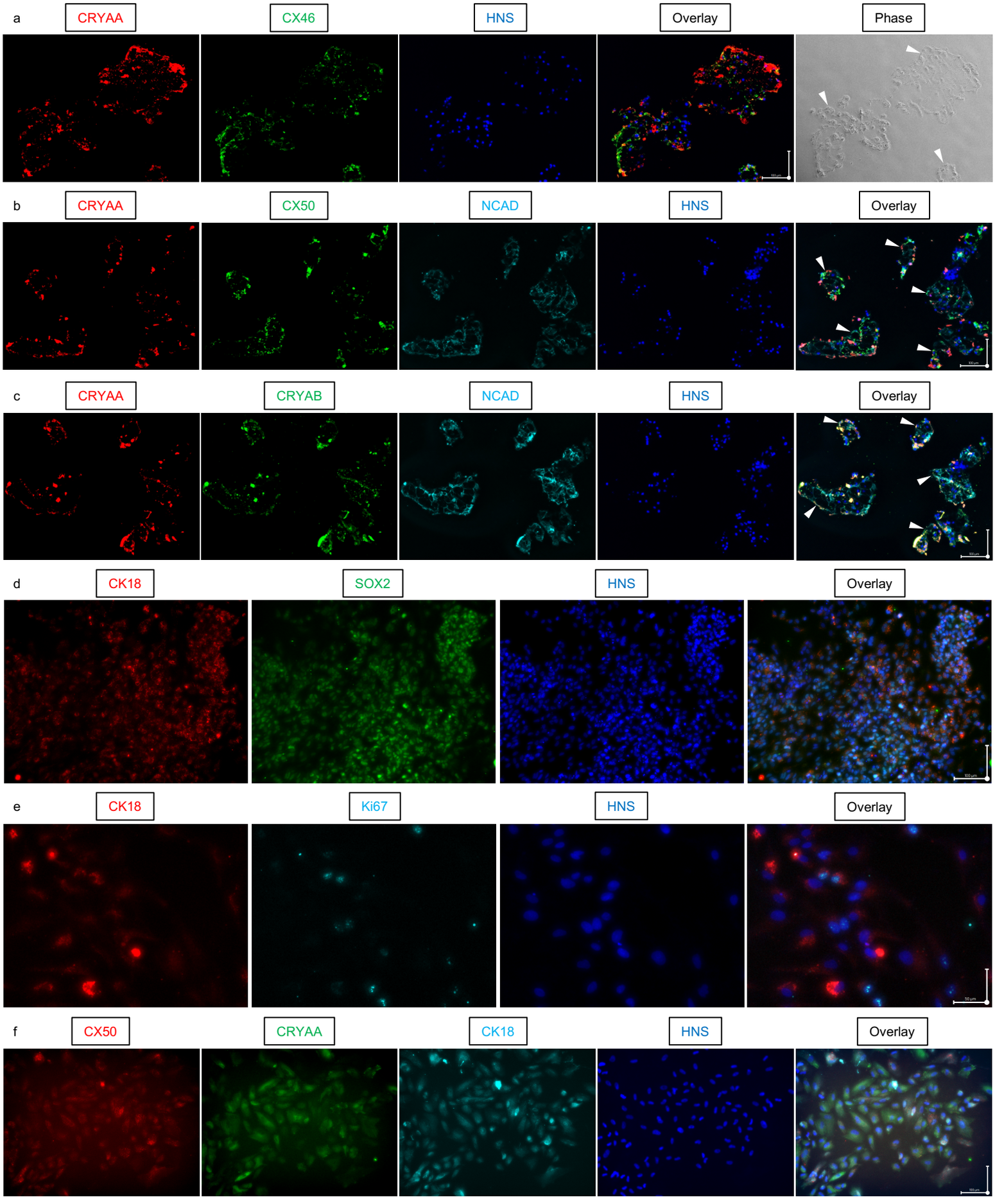

Supp. Fig. 7: Immunofluorescent localisation in isolated LOM (lens optimised medium) lentoid bodies (LBs), and in presumed human lens epithelia (LE) within LOM cultures at 3-4 weeks post-explantation of LB (evasion and expansion). a Isolated LB cryo-sections confirmed human CRYAA (red) and CX46 (green) within individual lentoids (white triangles), as-well-as CX50 (green) and NCAD (cyan) (**b**), and CRYAB and NCAD (cyan) (**c**); all with limited nuclei (HNS; blue). **d** Presumed LE confirmed human lens epithelial marker cytokeratin-18 (CK18; red) and pluripotency transcription factor SOX2 (green), and CK-18 (red) and proliferation protein Ki67 (cyan) (**e**). **f** Human lens -epithelium and -fiber marker CX50 (red), lens-related human crystallin CRYAA (green) and CK18 (cyan). Hoechst nuclei for all images (HNS; blue). Note: LE cells only, no lentoid bodies (**d** - **f**). Scalebars = 100μm and 50μm (**e**). *n*=3 independent biological replicates.

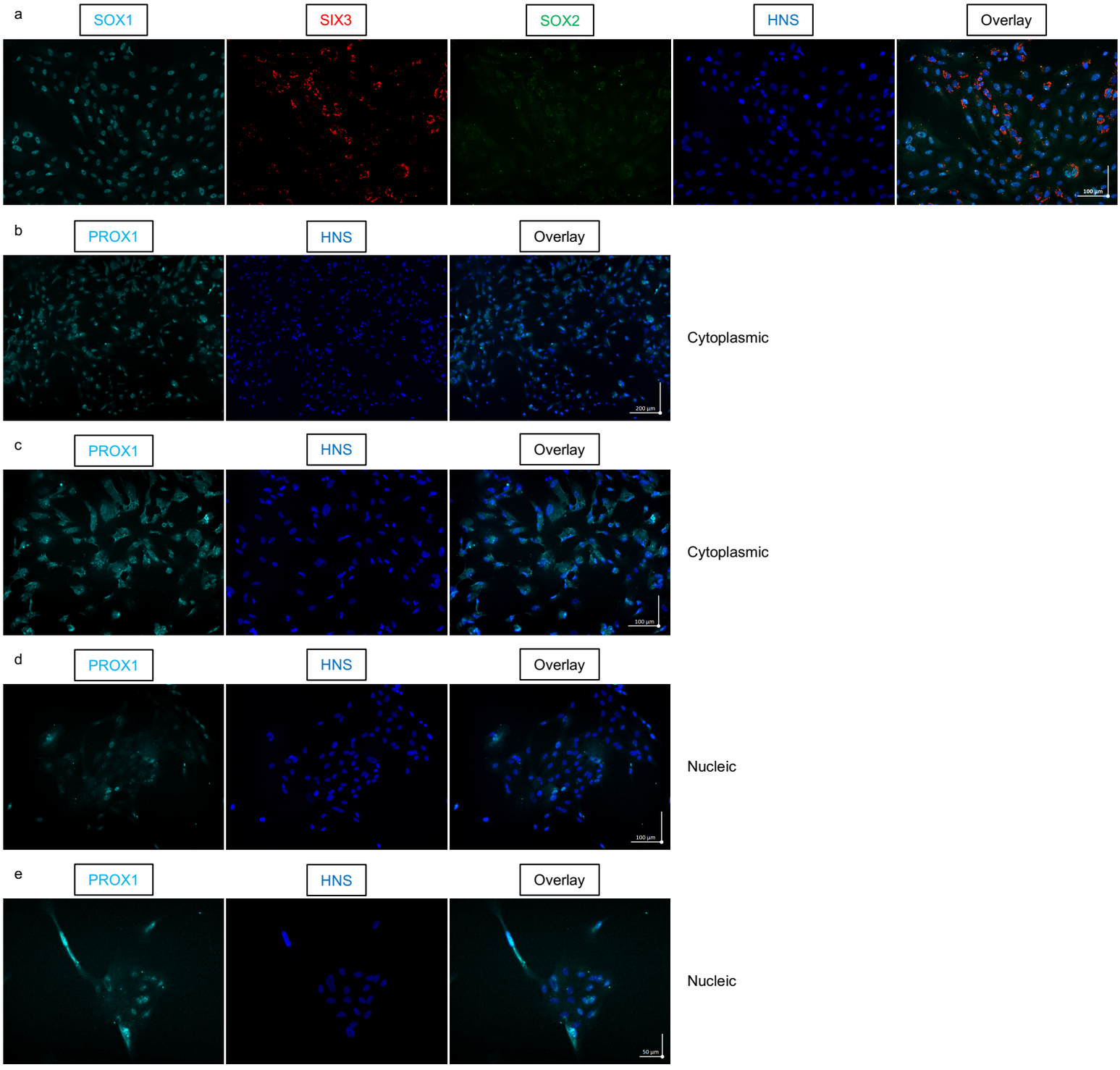

Supp. Fig. 8: Immunofluorescence identified lens-commitment crystallin differentiation transcription factors within passaged presumed lens epithelia (LE) cultures in LOM (lens optimised medium). When passaged LE from 8-week explanted lentoid bodies (LBs) were allowed to mature, lens-specification proteins underwent changes, as translocation of SIX3 to cytoplasm and significant loss of SOX2 (**a**). These same cultures also displayed lens-commitment proteins as SOX1-positive nuclei (**a**) and as PROX1-positive patterns within LE cytoplasm (**b**, **c**), and within nuclei of cells in close-contact areas (**d**, **e**) by translocation from cytoplasm in LE cells transitioning to lens fiber cells. Hoechst nuclei in images are blue (HNS). *n*=2 independent biological replicates.

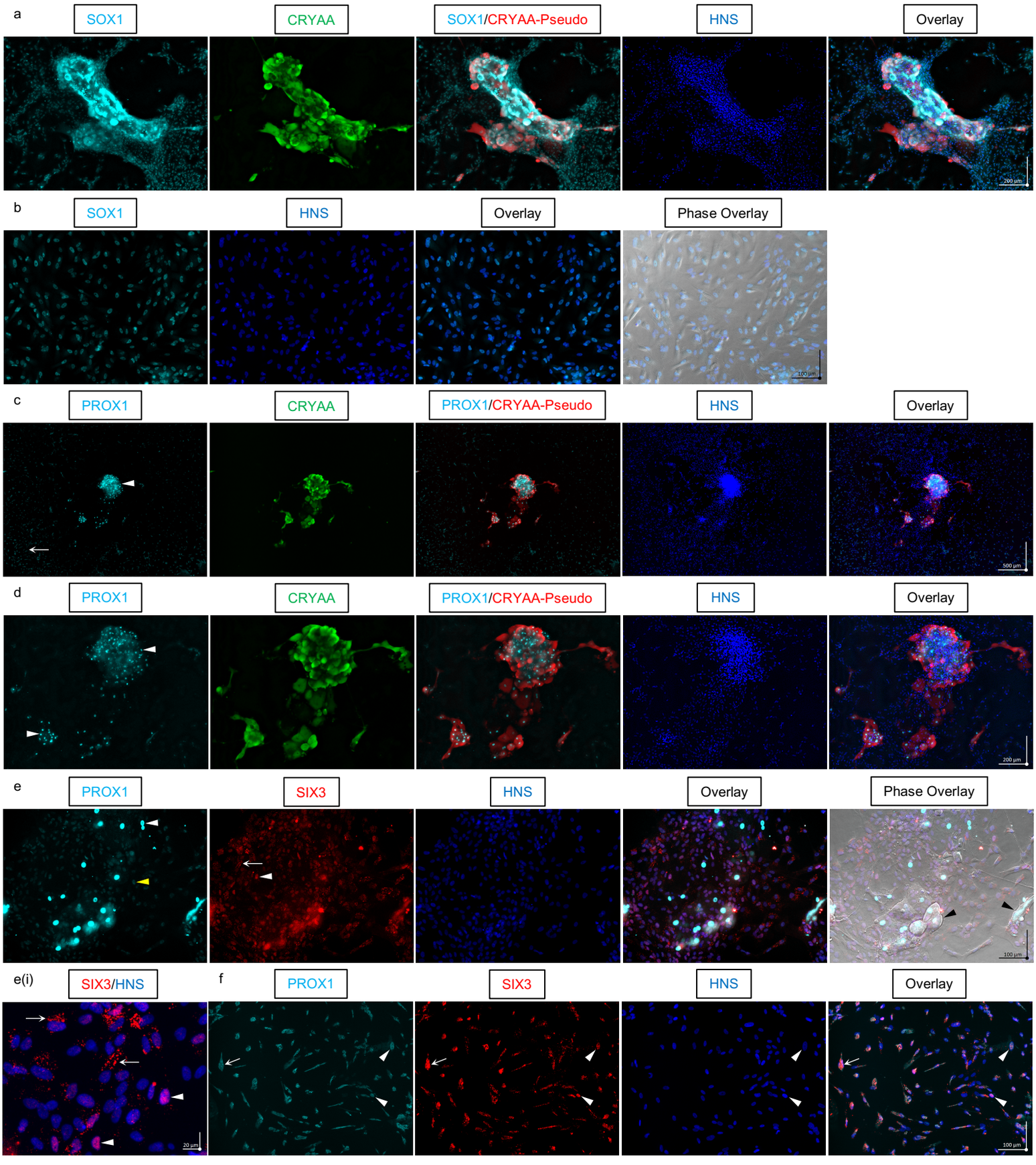

Supp. Fig. 9: Immunofluorescence identified lens-commitment crystallin differentiation transcription factors within older explanted lentoid bodies (LB) and evading presumed lens-epithelia (LE) in LOM (lens optimised medium). Isolated and explanted LBs from LOM cultures at 10 weeks displayed positive lens-commitment protein SOX1 (cyan) in nuclei (**a**) of CRYAA-positive lens fiber cells, as-well-as in nuclei of evaded LE cells (**b**), and significant loss of lens-specification protein SOX2. **c, d** LB lens fiber cells were CRYAA-positive (green/red-pseudo) with strongly concentrated PROX1-positive nuclei (cyan; white triangle) and weakly present in nuclei of surrounding CRYAA-negative LE cells (**e**), with clear cytoplasmic presence in evading LE cells (white arrow). **e** The LB explant showed strong (yellow triangle) PROX1-nuclear-positive cells (cyan), and immediately surrounding showed a mixed cellular population of weak (white triangle) PROX1-nuclear-positive cells (cyan), with SIX3-positive cells (red) in their nuclei (white arrow) and cytoplasm (white arrow; **e(i)**), similarly as in passaged mature LE cells (Supplementary Figure 8). PROX1-positive lens fibers displayed enlarged cell size and light-refraction properties under light-microscopy (black triangle). **e(i)** Example image of SIX3 nuclear and cytoplasmic locations at higher magnification and microscope zoom feature of (**e**). **f** At the LB explant culture periphery, the evaded LE cells were majorly positive for PROX1 and SIX3 within the cytoplasm, although positive-nuclei still existed. Hoechst nuclei in images are blue (HNS). *n*=2 independent biological replicates.

Supplementary Video

SI Video 1: Representative whole-well time-lapse imaging of hiPSCs from day 10 in StemFit until week 8 differentiation in ocular differentiation medium (ODM). Multiple SEAM (self-formed ectodermal autonomous multizone) colonies displayed dynamic morphological remodelling and limited lentoid induction with very small lentoids.

SI Video 2: Representative whole-well time-lapse imaging of hiPSCs from day 10 in StemFit until week 8 differentiation in lens optimised medium (LOM). Multiple SEAM (self-formed ectodermal autonomous multizone) colonies displayed dynamic morphological remodelling, with enhanced lens-zone expansion and lentoid induction as early as week 4, followed by continued lentoid expansion to week 8.

SI Video 3: Serial block-face scanning electron microscopy (SBF-SEM) flythrough of a LOM (lens optimised medium) lentoid after 8 weeks differentiation at a representative region of interest (ROI). SBF-SEM revealed lentoids as multilayered organoids of elongated presumed cortical lens fibers (LFs) that lacked obvious organelles and nuclei, and distinctive intercellular membranes between LFs that are characteristic of native lens cortex.

SI Video 4: Serial block-face scanning electron microscopy (SBF-SEM) 3D render of a LOM (lens optimised medium) lentoid after 8 weeks differentiation at a representative region of interest (ROI). SBF-SEM revealed lentoids as multilayered organoids of elongated presumed cortical lens fibers (LFs) that lacked obvious organelles and nuclei, and distinctive intercellular membranes between LFs that are characteristic of native lens cortex.

SI Video 5: Serial block-face scanning electron microscopy (SBF-SEM) flythrough of LOM (lens optimised medium) lentoid membrane interdigitations (MINTs) after 8 weeks differentiation at a representative region of interest (ROI). Distinctive intercellular membranes displayed well-defined MINTs resembling typical ball-and-socket structures, which resembled native lens fiber cortex morphology.

SI Video 6: Serial block-face scanning electron microscopy (SBF-SEM) flythrough of a LOM (lens optimised medium) lentoid after 8 weeks differentiation at additional regions of interest (ROIs). Some lentoid organoids were located subjacent to non-lenticular cells, in an opposed position to the presumed lens capsule, as expected in an ocular-population tissue culture model.

SI Video 7: Serial block-face scanning electron microscopy (SBF-SEM) 3D render of a LOM (lens optimised medium) lentoid after 8 weeks differentiation at additional regions of interest (ROIs). Some lentoid organoids were located subjacent to non-lenticular cells, in an opposed position to the presumed lens capsule, as expected in an ocular-population tissue culture model.

SI Video 8: Representative whole-well time-lapse imaging of explanted LOM (lens optimised medium) lentoid bodies (LBs) after 8 weeks differentiation. Explanted LOM LBs were subcultured on laminin-511 and in LOM from day 0 to day 21. LBs adhered and presumed lens-epithelia (LE) evaded and expanded outwardly from the explanted LBs.